Materials Science and Engineering B105 (2003) 126–131

www.elsevier.com/locate/mseb

New spectroscopic data of erbium ions in GaN thin films

F. Pellé [a,*], F. Auzel [a], J.M. Zavada [b], D.S. Lee [c], A.J. Steckl [c]

[a] *UMR7574-CNRS 1, Place Aristide Briand, F-92195 Meudon cedex, France*
[b] *US Army Research Office, Electronics Division, Durham, NC 27709, USA*
[c] *University of Cincinnati, Nanoelectronics Laboratory, Cincinnati, OH 45221, USA*

Abstract

Optical properties of erbium ions in MBE-grown GaN-thin films are reported. Three types of sites were identified using site selective laser excitation. The main center is ascribed to the Er^{3+} ions substituted in the Ga sub-lattice while the two other centers are assigned to Er-related defects. The lifetimes of the $^4S_{3/2}$ and $^4I_{13/2}$ multiplets of the main center are strongly quenched with increasing Er concentration. The complex decay profile of the visible fluorescence and its concentration dependence were modeled and interpreted using the diffusion-limited model. The dynamics of the infrared emission at 1.54 μm from the $^4I_{13/2}$ multiplet after excitation in the visible range is discussed. The crystal field strength of Er^{3+} in GaN was deduced from the overall crystal field splitting of the ground multiplet. Comparison of the results with those obtained in inorganic materials indicates that the rare earth is well embedded in the semiconductor host and not in a impurity oxide phase.

Keywords: Rare earth; GaN; Luminescence; Spectroscopy

1. Introduction

Visible emission of the RE^{3+} ions in Wide Band Gap Semiconductors (WBGS) are being intensively investigated. Among the wide-bandgap semiconductors, III-V nitrides seem to be the most promising host materials for RE^{3+} doping due to their energy band gap, which makes them transparent to the visible emission of RE^{3+}. Being chemically and thermally stable too, they are good candidates for optoelectronic and photonic applications. GaN is the most popular and new methods of synthesis (MOCVD and SSMBE) have allowed an increase in the incorporation of RE^{3+} into this material. Recent results obtained for RE^{3+}-doped GaN are very promising since GaN doped with Eu^{3+}, Tm^{3+} and Er^{3+} have been used to realize full-color electroluminescent devices [1]. Despite several studies of the spectroscopic properties of different RE^{3+} ions in GaN thin films, no clear correlation between the efficiency of the visible RE^{3+} luminescence and the interaction of RE^{3+} with the host has been established [2–4]. A complete understanding of the spectroscopic properties of the RE dopants in the semiconductor (excitation schemes and luminescence efficiency) and their relationship to growth processes is needed in order to improve the performance of current RE^{3+} doped GaN devices. In this paper, new results on the spectroscopic analysis of the Er^{3+} ions in GaN thin films are presented.

2. Experimental

The GaN:Er^{3+} thin films were grown using the Solid State Solid Source Molecular Beam Epitaxy (SSMBE) method on a p-type (1 1 1) Si substrate after deposition of an AlN buffer layer. The complete synthetic procedure is described in [5]. The Er^{3+} concentration of the GaN:Er^{3+} thin films, measured with Rutherford Backscattering Spectroscopy (RBS) and Secondary Ion Mass Spectroscopy (SIMS), ranges from 0.025 up to 11.2 at.%.

The Er^{3+}luminescence was excited either by an OPO pumped by the third harmonic of a pulsed Nd:YAG laser (501-DNS,720 BM Industrie) or by the Ar^+ lines at 514.5 and 496.5 nm (Coherent Innova 300). The luminescence was dispersed through a HR460 Jobin-Yvon monochromator and detected by a EMI 9558 QBM photomultiplier in the visible range and by a InGaAs (Hamamatsu) photodiode for the IR luminescence. Time resolved spectra and fluorescence

* Corresponding author. Tel.: +33-1450-75593; fax: +33-1450-75107.
E-mail address: pelle@cnrs-bellevue.fr (F. Pellé).

0921-5107/$ – see front matter © 2003 Elsevier B.V. All rights reserved.
doi:10.1016/j.mseb.2003.08.030

transients were digitized and averaged by an oscilloscope (TDS350 Tektronix) with data acquisition on a PC. Low temperature measurements were performed by cooling the samples in a closed-cycle CTI cooling system.

3. Photoluminescence properties

3.1. Luminescence at room temperature

Excitation of the Er^{3+} ions within the GaN band gap (to the $^4F_{7/2}$ or $^2H_{11/2}$ multiplets) yields a luminescence spectrum dominated at room temperature by emission in the visible range. This is easily assigned to radiative transitions from the $^2H_{11/2}$ and $^4S_{3/2}$ multiplets to the ground state one. Weak transitions from the lower multiplets ($^4F_{9/2}$, $^4I_{9/2}$, $^4I_{13/2}$) are observed, too (Fig. 1). Emission from the $^4I_{13/2}$ multiplet shows a rather high efficiency compared to that observed from the $^4F_{9/2}$ and $^4I_{9/2}$ multiplets. No significant changes in the luminescence are observed with increasing Er^{3+} concentration and the luminescence from the $^4S_{3/2}$ and $^4I_{13/2}$ multiplets have the same behavior with a maximum intensity at about 1 at.% in both cases. Non-exponential decay and the concentration dependence of the $^4S_{3/2}$ emission indicate that the optical relaxation involves energy transfer between adjacent Er^{3+} ions (Fig. 2).

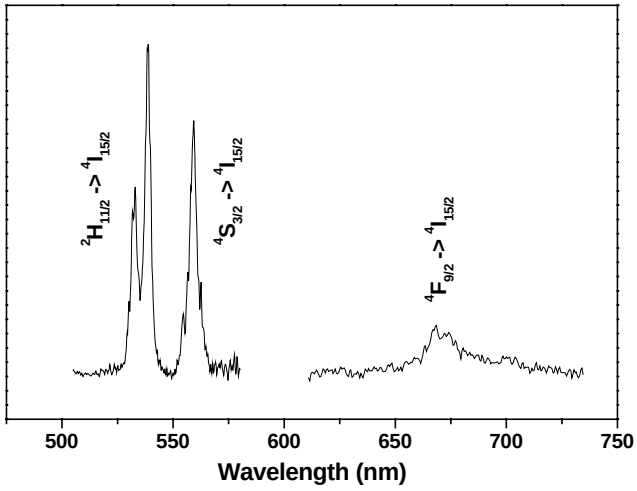

Fig. 1. Visible fluorescence spectrum of GaN: Er^{3+} (0.17 at.%) recorded at room temperature under resonant excitation in the $^4F_{7/2}$ multiplet ($\lambda_{excitation} = 498$ nm).

3.2. Infrared emission: selective excitation

The selective excitation spectra at low temperature ($T = 10$ K) were analyzed monitoring the $^4I_{13/2} \rightarrow {}^4I_{15/2}$ main emission lines (Fig. 3a). The most intense lines at 1531 and 1537 nm are observed only when excited in the $^2H_{11/2}$ multiplet (Fig. 3b) The two other lines at 1545 and 1552 nm are only weakly excited from the $^2H_{11/2}$ multiplet but another efficient excitation line is observed at 515.7 and 518 nm, respectively. These lines fall off the resonance with the intra-configurational 4f transitions of Er^{3+} (Fig. 3b). The three different infrared emission spectra recorded with selective excitation (Fig. 3a) were ascribed to different emitting centers labeled as C1, C2 and C3. Selective excitation into the two lines observed around 516 nm provides emission of one order of magnitude higher intensity than when excited into the intra configuration 4f transitions. In these cases, the luminescence is mainly due to the transition between the lowest levels of the $^4I_{13/2}$ and $^4I_{15/2}$ manifolds. The transitions to other Stark components of the ground state being very weak, a complete analysis of the level schemes cannot be performed. The emission spectrum and its temporal behavior strongly depend on the excitation wavelength. Furthermore,

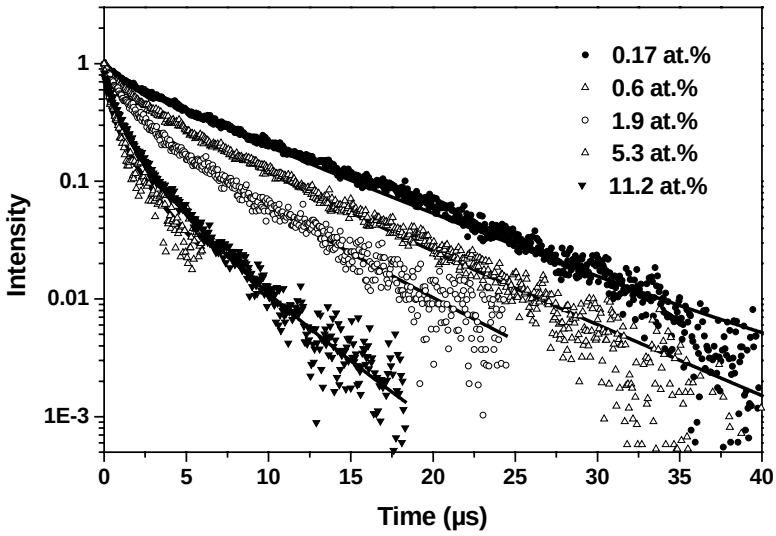

Fig. 2. $^4S_{3/2}$ decay profile as a function of Er^{3+} concentration ($T = 300$ K) (symbols: experimental data; full lines: theoretical curves calculated using Eq. (1).

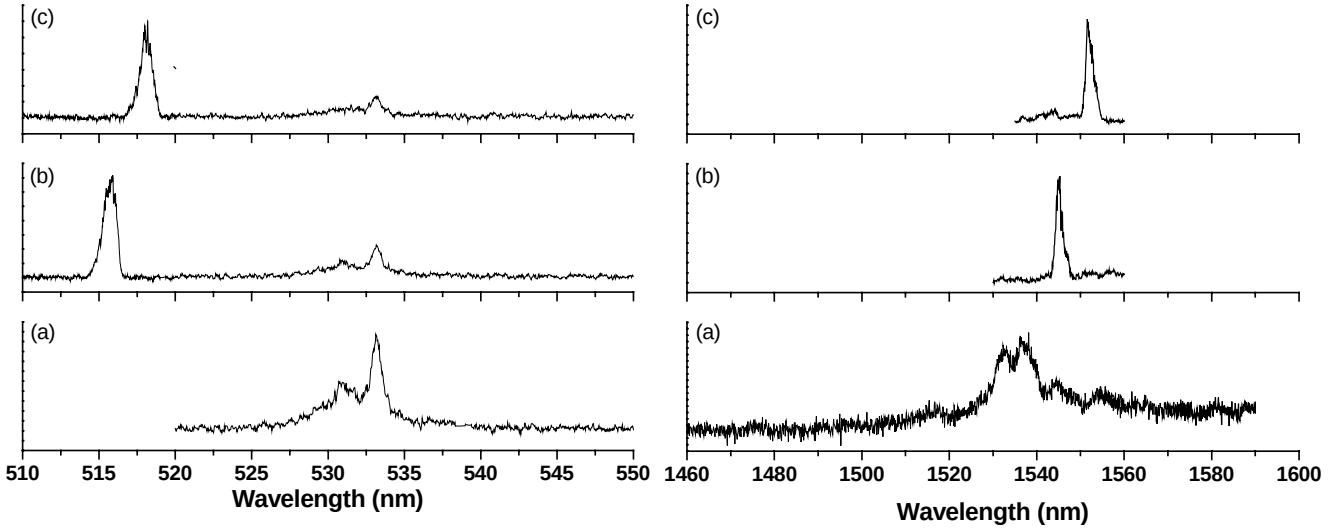

Fig. 3. (A) Selective excitation spectrum of the $^4I_{13/2} \rightarrow {}^4I_{15/2}$ transition recorded at 10 K for GaN:Er^{3+} (0.6 at.%): (a) $\lambda_{analysis} = 1537$ nm; (b) $\lambda_{analysis} = 1545$ nm; (c) $\lambda_{analysis} = 1552$ nm. (B) $^4I_{13/2} \rightarrow {}^4I_{15/2}$ fluorescence spectrum recorded at 10 K for GaN:Er^{3+} (0.6 at.%) with selective excitation: (a) $\lambda_{excitation} = 533.7$ nm; (b) $\lambda_{excitation} = 515.7$ nm; © $\lambda_{excitation} = 518$ nm.

Table 1
$^4I_{13/2}$ rise and decay times measured at 10 K for the different centers (GaN: 0.6 at.% Er^{3+})

	$\lambda_{excitation}$ (nm)	Rise time (μs)	Decay time (ms)
C1	533.7	862	3.1
C2	515.7	64.5	1.718
C3	518	79	1.773

with increasing temperature, the intensity of the C2 and C3 luminescence decreases greatly and cannot be recorded.

The luminescence intensity of the selectively excited $^4I_{13/2}$ multiplet as a function of time (Fig. 4) shows that the time constants of the excitation as well as the decay processes for center C1 are much longer than those for C2 and C3. These processes have been modeled using a simple model with a rise (τ_r) and exponential decay (τ_d). The time constants deduced from the theoretical fit of the experimental curves (Table 1) indicate that the processes involved in the population and de-excitation of the $^4I_{13/2}$ multiplet of centers C2 and C3 are quite identical. This indicates a similar environment of the Er^{3+} ions in C2 and C3.

The luminescence decay curves of the $^4I_{13/2}$ multiplet for the center C1 measured at room temperature as a function of Er^{3+} concentration reveal that the both decay and rise times (Table 2) are strongly reduced with increasing Er^{3+} content as a consequence of Er^{3+}–Er^{3+} interactions.

Table 2
$^4I_{13/2}$ rise and decay times measured at room temperature as a function of Er^{3+} concentration ($\lambda_{excitation} = 533.7$ nm, analysis for center C1 at $\lambda_{analysis} = 1537$ nm)

[Er^{3+}] (at.%)	Rise time (μs)	Decay time (ms)
0.17	98	2.43
0.6	33.6	1.41
1.9	21	0.310

4. Identification of the emitting centers

The occurrence of several centers for Er^{3+} ions and excitation of the $^4I_{13/2}$ multiplet within the GaN band gap and out of the absorption range of the Er^{3+} ($^{2S+1}L_J$) states of the $4f^{11}$ configuration has already been reported for the Er-implanted GaN thin films [6,7]. The excitation spectrum consisted of an unstructured broad band extending from 460 to 530 nm. The present additional excitation lines are well within this broad band and the shape of the C2 and C3 emission spectra are very similar to those in [6]. The doping by implantation [6] causes damage in the GaN lattice that cannot be completely removed by annealing. A high concentration of defects or the presence of extended defects is expected in the implanted samples. This may explain the broad band observed previously when compared to the present samples obtained by MBE in which the defects should be more localized, giving rise to discrete spectra. The luminescence intensity obtained by the non-intraconfigurational 4f excitation is of an order of magnitude more intense than that recorded with resonant 4f–4f excitation ([6] and this work). The high efficiency of the extra excitation and the very low absorption cross sections of the intra-configurational 4f transitions suggest that the excitation of the C2 and C3 centers proceeds by an Er^{3+} trap-related absorption rather than via 4f–4f transitions of Er^{3+}. No visible or infrared emission from these centers was recorded with direct excitation in the 4f–4f transitions. Despite lower infrared emission intensity for C1, this center can be directly excited by the very weak 4f–4f transitions. The concentration of

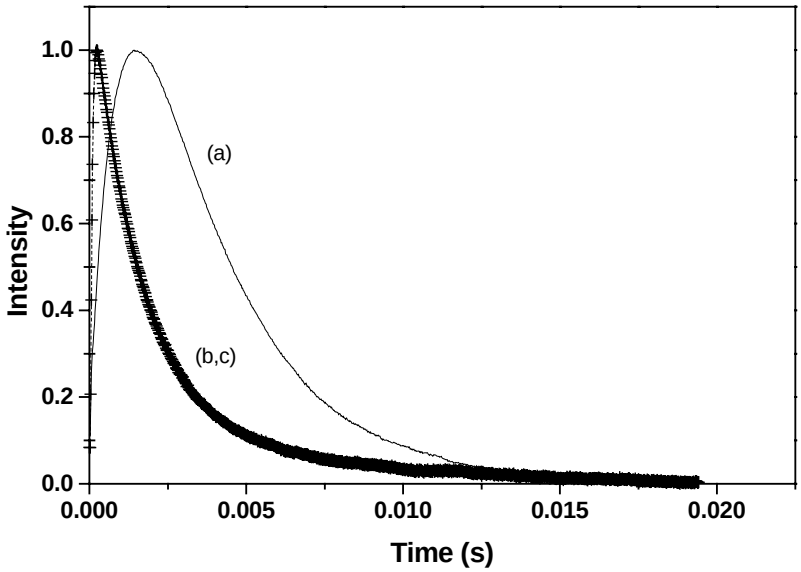

Fig. 4. $^4I_{13/2}$ decay profile as a function of excitation wavelength recorded at 10 K: (a) $\lambda_{excitation} = 533.7$ nm and $\lambda_{analysis} = 1537$ nm corresponding to C1; (b) $\lambda_{excitation} = 515.7$ nm and: $\lambda_{analysis} = 1545$ nm corresponding to C2; © $\lambda_{excitation} = 518$ nm and $\lambda_{analysis} = 1552$ nm corresponding to C3 (full line: theoretical fit; cross: experimental curves).

the C2 and C3 centers must thus be much lower than that of C1.

The non-exponential time dependence and the concentration dependence of the visible luminescence suggest an important contribution from the Er^{3+}–Er^{3+} interactions to the de-excitation process for the center C1. Based on RBS analyses it was found that a great majority (≈95%) of the Er^{3+} ions occupies substitutional sites in the Ga sublattice even at relatively high Er^{3+} concentration [8]. At very high Er^{3+} concentration, a pure ErN phase is obtained as shown by XRD demonstrating also the clustering of Er^{3+} in GaN [5]. The concentration quenching of the lifetime (Fig. 3) indicates that a cluster formation is present even at low Er^{3+} concentrations. Based on the spectroscopic data and the XRD patterns as a function of the Er^{3+} content, the C1 center is ascribed to the Er^{3+} ions in the regular Ga site. The C2 and C3 centers can be attributed to Er^{3+} ions in interstitial positions near defects produced by introducing the dopants into the lattice, as observed for other RE^{3+} doped semiconductors. RE^{3+} induced levels in the band gap and their role in the excitation process have already been shown for InP:Yb^{3+} [9], GaAs:Er^{3+} [10] and Er^{3+}:Si [11].

5. Luminescence dynamics

5.1. Visible emission of the C1 center

The C1 center can be considered as the main center. The time dependence of the $^4S_{3/2} \rightarrow {}^4I_{15/2}$ luminescence at room temperature deviates from a simple exponential behavior irrespective of the Er^{3+} concentration (Fig. 3). For low Er^{3+} concentrations, the decay profile can be fitted to two exponential functions explained by the presence of two Er^{3+} sites. For high Er^{3+} concentrations, the experimental decay curves cannot be fitted by only two exponentials indicating that other processes such as energy transfer and/or diffusion are involved. The deviation from the simple exponential law in the initial part of the decay increases with increasing Er^{3+} concentration. The long part of the decay follows an exponential behavior with a time constant which gradually decreases with increasing the Er^{3+} concentration. For even higher Er^{3+} concentrations, the overall decay of the $^4S_{3/2}$ luminescence becomes faster and approaches to a single exponential decay (Fig. 2). The ion-ion interactions should be taken into account to explain the decay profile and the strong decrease in the decay time with increasing Er^{3+} concentration. Since no impurity has been detected, Er^{3+} will be considered as both a sensitizer and an activator. From the concentration dependence of the asymptotic decay, the experimental decay curves were interpreted according to the diffusion limited model. A general solution has been obtained for the sensitizer decay function including diffusion within the sensitizer system and sensitizer–acceptor energy transfer via a dipole–dipole coupling [12]:

$$I(t) = I(0)\exp\left[-\frac{t}{\tau_0} - \frac{4\pi^{3/2}}{3}N_A(\alpha_{SA}t)^{1/2} \times \left(\frac{1+10.87x+15.50x^2}{1+8.743x}\right)^{3/4}\right] \quad (1)$$

where $x = D\alpha_{SA}^{-1/3}t^{2/3}$, with D and N_A the diffusion constant and the acceptor concentration, respectively and α_{SA} is related to the sensitizer–acceptor interaction. The calculations are described in detail elsewhere [13]. All the microscopic parameters characterizing the Er^{3+}–Er^{3+} interaction

in different GaN samples were determined. The calculated curves using Eq. (1) agree well with the experimental data.

5.2. Infrared emission

The complex decay behavior of the visible emission allows one to deduce the strong Er^{3+}–Er^{3+} interactions for C1. Because of the weak intensity of the transitions from levels between the excited multiplet ($^4S_{3/2}$) and $^4I_{13/2}$, the multiphonon relaxation process seems not very efficient. The population of the $^4I_{13/2}$ multiplet of C1 can be explained by a cross relaxation process which overcomes the multiphonon relaxation. The first step of the relaxation of the visible excitation proposed is the ($^4S_{3/2}$, $^4I_{15/2}$) → ($^4I_{11/2}$, $^4I_{13/2}$) cross relaxation after a migration of the excitation within the $^4S_{3/2}$ multiplet. In a second step, the $^4I_{13/2}$ multiplet is populated by the $^4I_{11/2} \rightarrow {}^4I_{13/2}$ radiative transition since at 10 K the probability of the $^4I_{11/2} \rightarrow {}^4I_{13/2}$ multiphonon process is very low.

The process populating the emitting $^4I_{13/2}$ level of the C2 and C3 centers is faster, but a similar cross relaxation process between the related trap excited level and the $^4I_{13/2}$ level is proposed. This can explain why no emission from the $^4S_{3/2}$ level can be observed.

5.3. Self quenching of the infrared emission of C1 center

The quenching of the infrared emission with increasing Er^{3+} concentration (Table 2) cannot be due to a cross relaxation process, since the $^4I_{13/2}$ emitting state is the first excited state. However, the self-quenching behavior is still well described by a limited diffusion process [14]. The quenching centers are most probably the C2, C3 centers which levels are at energy below that of C1. The corresponding intrinsic decay $\tau_0(^4I_{13/2})$ was found to be 2.48 ms, and the critical concentration N_0 equal to 0.67×10^{21} cm^{-3} (0.8 at.%).

The quantum efficiency of the infrared emission was estimated by comparison with the results obtained for a fluoride glass using the same phonon cut-off frequency and similar crystal field strength. After correction for the index of refraction, the quantum efficiency for the 1.5 μm emission was found to be 77 and 62.5% at low temperature and at room temperature, respectively. The energy transfer to free carriers could explain the lower quantum efficiency in GaN than in an insulator such as YAG.

6. Crystal field strength analysis

Based on the emission spectra recorded for different C1 excited multiplets, the energies of the Stark components and the overall splitting of the ground multiplet were deduced. From the overall splitting of the $4f^N$ multiplets, it is possible to deduce the crystal field (CF) strength using a scalar field parameter N_v which allows a convenient comparison between different host materials [15]. The overall splitting of the ground $^4I_{15/2}$ multiplet (299 cm^{-1}) gives 1557 cm^{-1} for the N_v value that is between those for $CsCdBr_3$ and $LiYF_4$ known as materials with weak crystal field. Calculation of the CF strength expected for Nd^{3+} (no reliable N_v values are available for Er^{3+}) is possible by taking into account the lanthanide contraction [16]. The $N_v(Nd^{3+})$ value for GaN (2139 cm^{-1}) is between those for $LaCl_3$ (1062 cm^{-1}) and LaF_3 (2356 cm^{-1}). The CF strength in GaN is much weaker than in oxides for which the N_v value is larger than 3000 cm^{-1} [17]. This indicates that the rare earth is well imbedded in the semiconductor host and not in an impurity oxide phase. On the other hand, a comparison to the results for GaAs: Er^{3+} [17], the overall splitting for $^4I_{13/2}$ (353 cm^{-1}) in GaAs would give a much higher N_v value (2504 cm^{-1}) in agreement with oxygen surrounding the Er^{3+} [18]. Since N_v for Er^{3+} in GaN is clearly lower than that for GaAs or the oxide hosts, the present results suggest the substitution of Ga^{3+} by Er^{3+}.

Another way to verify this hypothesis is to study the nephelauxetic red shift [19] of the $^4I_{13/2} \rightarrow {}^4I_{15/2}$ transition barycenter at 1.5 μm for various Er^{3+} doped materials available in the literature data [18,20,21]. The barycenter $^4I_{13/2} \rightarrow 4I_{15/2}$ value (6462 cm^{-1}) for GaN is between those for YAG and $CsCdBr_3$ which corresponds to a covalent surrounding for R^{3+} ions. The electronic environment of Er^{3+} in GaN is thus rather covalent. As a conclusion, a comparison with the results for GaAs centers with oxygen and with strong crystal field, the C_1 main center in GaN shows a typical behavior to be expected for a Ga site with covalent bonding to nitrogen: a weak crystal field and a large nephelauxetic red shift.

7. Conclusions

Based on site-selective excitation spectroscopy, three kinds of sites were identified for the Er^{3+} ions in GaN. The main center was concluded to be Er located on the Ga site. The majority of the Er^{3+} ions are in this center. The two other sites were assigned to Er^{3+}-related defects and ascribed to Er^{3+} species in interstitial positions. A non-exponential decay profile and the concentration dependence of the $^4S_{3/2}$ luminescence for the main center indicate that the optical relaxation involves energy transfer processes between adjacent Er^{3+} ions. The luminescence decay curves were modeled and interpreted using a diffusion-limited migration of the optical excitation. All the microscopic parameters characterizing the interaction were determined and compared to the experimental data. The quenching of the infrared luminescence is found to occur due to the same process. Acceptors could be identified as centers ascribed to Er^{3+} in interstitial positions. The crystal field strength parameter was calculated for Er^{3+} in the main center and compared to that in other inorganic materials. The results confirm the substitution of the rare earth ion in

the semiconductor crystal excluding oxygen environment. This is supported by the covalent character of the bonding of Er^{3+} to nitrogen for the main center.

Acknowledgements

This material is based upon work partially supported by the European Research Office of the US Army under contract No N62558-02-M-5113. Mrs Gardant is acknowledged for her assistance.

References

[1] D.S. Lee, J. Heikenfeld, R. Birkhahn, M. Garter, B.K. Lee, A.J. Steckl, Appl. Phys. Lett. 76 (2000) 1525.
[2] U. Hömmerich, J.T. Seo, J.D. MacKenzie, C.R. Abernathy, R. Birkhahn, A.J. Steckl, J.M. Zavada, in: Proceedings of MRS Fall 1999 Meeting, MRS Internet J. Nitride Semicond. Res. 5S1, W11.65 (2000).
[3] U. Hömmerich, J.T. Seo, M. Thaik, J.D. MacKenzie, C.R. Abernathy, S.J. Pearton, R.G. Wilson, J.M. Zavada, Internet J. Nitride Semicond. Res. 4S1 (1999) G11.6.
[4] A.J. Steckl, R. Birkhahn, Appl. Phys. Lett. 73 (1998) 1702.
[5] D.S. Lee, J. Heikenfeld, A.J. Steckl, U. Hömmerich, J.T. Seo, A. Braud, J.M. Zavada, Appl. Phys. Lett. 79 (2001) 719.
[6] H. Przybyliñska, A. Kozanecki, V. Glukhanyuk, W. Jantsch, D.J. As, K. Lischka, Physica B 308 (2001) 34.
[7] T. Monteiro, J. Soares, E. Alves, J. Appl. Phys. 89 (2001) 6183.
[8] K. Lorenz, R. Vianden, R.H. Birkhahn, A.J. Steckl, M.F. Da Silva, J.C. Soares, E. Alves, Nucl. Instr. Meth. B 161/163 (2000) 946.
[9] K. Takahei, A. Taguchi, H. Nakagome, K. Uwai, P.S. Whitney, J. Appl. Phys. 66 (1989) 4941.
[10] R.A. Hogg, K. Takahei, A. Taguchi, Phys. Rev. B 56 (1997) 10255.
[11] F.P. Widdershoven, J.P.M. Naus, Mater. Sci. Eng. B 4 (1989) 71.
[12] M. Yokota, O. Tanimoto, J. Phys. Soc. Japan 22 (1967) 779.
[13] F. Pellé, F. Auzel, J.M. Zavada, U. Hömmerich, D.S. Lee, A.J. Steckl, Nato Sciences Series, NATO Sciences Series II: Mathematics, Physics and Chemistry, vol 126, 1 (2003).
[14] F. Auzel, F. Bonfigli, S. Gagliari, G. Baldacchini, J. Lumin. 94-95 (2001) 293.
[15] F. Auzel, O. Malta, J. Phys. (Fr.) 44 (1983) 201.
[16] F. Auzel, Opt. Mater. 19 (2002) 89.
[17] E. Antic-Fidancev, J. Hölsä, M. Lastusaari, A. Lupei, Phys. Rev. B 64 (2001) 195108.
[18] H. Hennen, J. Schneider, G. Pomerenke, P.C. Becker, Appl. Phys. Lett. 43 (1983) 943.
[19] C.K. Jorgensen, Prog. Inorg. Chem. 4 (1962) 73.
[20] A.A. Kaminskii, Laser Crystals: Their physics and properties, Springer, Berlin, 1990.
[21] N.J. Cockroft, G.D. Jones, R.W.G. Syme, J. Lumin. 43 (1989) 275.